Laser spectroscopic measurement of point-defect dynamics in Eu^{3+}:CaF_2

Kathleen M. Cirillo-Penn* and John C. Wright†

Department of Chemistry, University of Wisconsin–Madison, 1101 University Avenue, Madison, Wisconsin 53706

(Received 10 January 1990)

We have developed a site-selective laser method to study the aggregation kinetics of defect sites as a result of heat treatment in EuF_3-doped CaF_2 crystals. The crystals contain Eu^{3+} in four dominant defect sites and one minor site that differ in the number of nearby dopant and fluoride interstitial ions. A nonequilibrium site distribution was created by quenching the high-temperature distribution. The kinetics of the reequilibration to a lower-temperature distribution was followed by measuring the absolute concentrations of the defect sites with site-selective laser spectroscopy. The functionality of the temporal changes, the absolute concentrations, and the concentration and temperature dependence of the rate constants have been used to definitively identify the four major sites and to quantitatively describe the entire behavior of the defect distributions. The four sites are identified as an isolated Eu^{3+}; a single-pair site of a Eu^{3+} ion and a compensating fluoride interstitial; a dimer consisting of two Eu^{3+} ions, no fluoride vacancies, two displaced fluoride ions, and three fluoride interstitials $(2|0|2|3_1)$; and a trimer of three Eu^{3+} ions and four fluoride interstitials $(3|0|2|4_1)$. It is suggested that the trimer and dimer are related to the hexamer clusters observed with heavier rare-earth dopants and that the hexamers contain extra fluoride interstitials that form a series of clusters with the largest possible cluster being $6|0|32|12$. We also determined activation energies of 0.49 ± 0.08 eV and 1.5 ± 0.4 eV for the formation of the dimer and trimer, respectively. This work presents the first complete microscopic picture for the solid-state defect chemistry of a fluorite material. It is in agreement with recent predictions of HADES (Harwell Automatic Defect Examination System) models for fluorite defect centers.

I. INTRODUCTION

In the past 25 years many groups have studied the problems of aliovalent defects in ionic crystals. In particular, much work has sought to understand the nature of trivalent rare-earth defects in fluorite systems since these serve as important models in the study of defects in solids.[1-3] Lightly doped calcium fluoride is frequently cited as a system that displays the classical defect behavior of ionic solids.[4,5] Its simple fluorite lattice has made it popular as a test case for defect computations, both because of the interest in the fluorite system[6-15] and the justification for extending the methods to more complex systems.[16] Since the fluorite structure is the simplest crystal structure to exhibit fast-ion conduction, calcium fluoride is also used to test theoretical ion conduction models.[17,18]

Trivalent rare-earth dopants in CaF_2 are charge compensated by either fluoride interstitials that are so distant that the dopant has cubic symmetry or are near enough to change the local symmetry.[19] Since many configurations are possible with nearby compensation, a large effort has been required to identify the actual configurations and to establish the defect equilibria that control the distribution of the defect centers. Figure 1 shows the sites proposed for the dominant centers in this work along with the cubo-octahedral cluster mentioned later. The simplest centers are single pairs that involve one rare-earth ion compensated in either a near-neighbor (NN) or next-nearest-neighbor (NNN) position by a

fluoride interstitial ion, F_i', to give sites of C_{4v} or C_{3v} point-group symmetry.[19] Only the tetragonal site is present for lighter-rare-earth dopants while both are present for heavier dopants.[7] These sites are identified by the notation of Corish *et al.* as $1|0|0|1_1$ and $1|0|0|1_2$, respectively, where the four numbers represent the number of dopant cations, fluoride vacancies, displaced lattice fluoride ions, and fluoride interstitial ions, respectively.[11] The subscript on the last number indicates a NN or NNN F_i'. Traditional descriptions of defect equilibria in fluorites assume a pairing equilibrium between cubic sites and F_i' that determines the number of free F_i' seen in conductivity experiments.[20] We write

$$1|0|0|0 + 0|0|0|1 \rightleftharpoons 1|0|0|1 \ .$$

Although a mass-action description of this equilibrium fits conductivity measurements, a number of studies show the actual site distribution does not follow a mass-action relationship.[21-28] The cubic site increases relative to the single-pair sites as the dopant concentration is raised and it decreases as the annealing temperature is raised. Mass-action relationships predict that a higher dopant concentration would raise the F_i' concentration so the cubic sites would be suppressed relative to single pairs. Similarly, higher annealing temperatures would raise both the F_i' and cubic site concentrations by dissociation of the single pairs.

Two models have been advanced to explain the anomalies. The presence of other centers with extra F_i' ions and effective negative charges can provide compet-

ing equilibria for F_i' (Refs. 21–25) or Coulombic and strain interactions can cause enough shielding effects to make nonideality corrections or activity effects dominant.[28–30] There is good evidence for both explanations. Calculations have predicted the importance of $1|0|1|2_1$, $2|0|2|2_1$, $2|0|2|3_1$, $3|0|1|3_1$, $4|1|2|4_1$, $4|0|8|4_1$, $6|0|8|4_1$, $6|0|8|5_1$, and $6|0|8|6_1$ clusters.[6,8,10–13,15,31] The hexamer clusters were predicted for rare earths heavier than Gd^{3+} and dimers were predicted to dominate for lighter rare earths.[31] The centers with excess F_i' ions could be formed by either scavenging or gettering them from single pairs or by a disproportionation reaction:

$$1|0|0|1 + 2|0|2|2 \rightleftharpoons 1|0|0|0 + 2|0|2|3 ,$$

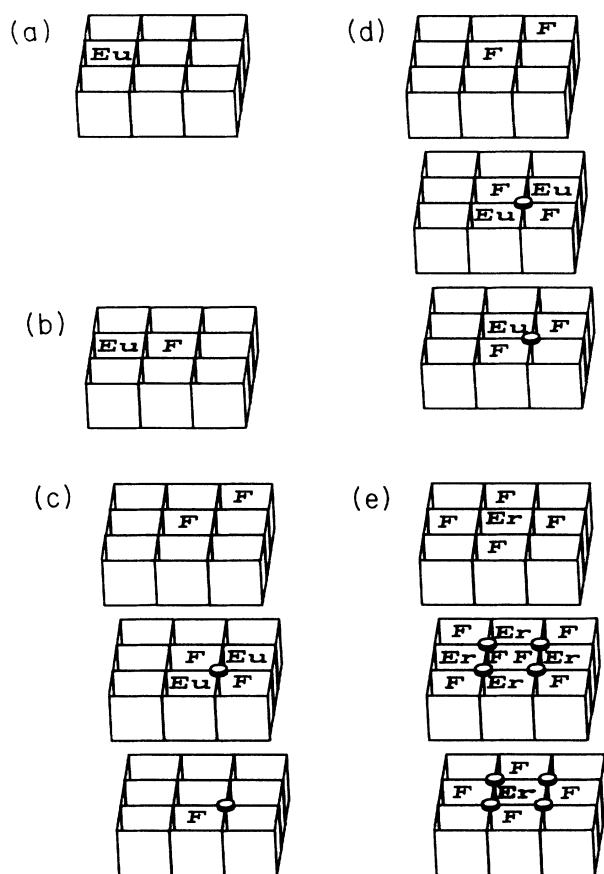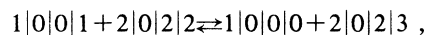$$2(2|0|2|2) \rightleftharpoons 2|0|1|2 + 2|0|2|3 .$$

FIG. 1. Exploded three-dimensional representation of the Eu^{3+} defect centers found in this work [(a)–(d)] and the cubo-octahedral center of heavier dopants like Er^{3+} (e). Three-dimensional line intersections represent normal fluoride lattice sites while Ca^{2+} ions (not shown) occupy alternate cube center positions. The fluoride interstitial and Eu^{3+} ions are shown explicitly for the different defects. Fluoride vacancies are indicated by disks at line intersections. (a) Cubic center, O site; (b) tetragonal single-pair site, A site; (c) $2|0|2|3_1$ center, R site; (d) $3|0|2|4_1$ center, Q site; (e) $6|0|8|6_1$ cubo-octahedral center, proposed for Er^{3+} dopant.

Both reactions were expected to be important[12] but only the first reaction would explain the fluorites' anomalous concentration and temperature dependences. Calculations show there is a strong tendency for F_i' trapping to form either $1|0|1|2$ or $2|0|2|3$ centers.[10–12]

Experimental work is in agreement with this picture. Site-selective laser spectroscopy has been performed in CaF_2 doped with light ions like Eu^{3+} (Ref. 27) and heavier ions like Er^{3+}.[26] Eu^{3+} has four-dominant sites— a cubic site, a single-pair tetragonal site, and two clusters labeled R and Q. Er^{3+} has many sites—a cubic site, tetragonal and trigonal single-pair sites, a dimer site labeled C, and two families of clusters associated with sites that have been labeled $D(1a) \rightarrow D$ (1k) and $D(2a) \rightarrow D(2d)$. The C site was shown to be correlated with F_i' scavenging because the C site decreased in concentration as the annealing temperature increased over the range where the anomaly in the cubic–to–single-pair ratio occurred.[32] The $D(2)$ family of clusters was shown to correspond to the cubo-octahedral $6|0|8|6$ cluster[32] by correlations with experiments performed by Greis and co-workers.[33–35] They performed x-ray measurements at high dopant concentrations of the heavier rare earths in samples that had been annealed for an extended time and showed that cubo-octahedral $6|0|8|6_1$ clusters form superstructures within the fluorite lattice. Since the $D(2)$ family of clusters is the dominant feature at high dopant concentrations, they are expected to correspond to the $6|0|8|6_1$ clusters. Extended x-ray-absorption fine structure (EXAFS) measurements of heavily doped samples confirmed that the cubo-octahedral $6|0|8|6$ clusters are the stable species for the heavier-rare-earth dopants.[15,31] The measurements also indicated that the $2|0|2|3_1$ dimers are the stable clusters for the lighter rare earths.

There has been speculation about the role of the $1|0|1|2$ center in the fluorites.[11,36,37] The species is important because it could be the factor determining the anomalous concentration and temperature dependences of the defect distributions. HADES (Harwell Automatic Defect Examination System) calculations show it should be a stable species.[11] Welsh suggested that the trigonal single-pair site observed in the optical spectroscopy or the dielectric relaxation actually was the $1|0|1|2_1$ center but there have been no experiments that have identified it.[36]

The second explanation for the anomalous concentration and temperature dependences is that strain interactions augment Coulombic interactions between charged defect species so there is a greater association than would be predicted from simple mass-action relationships.[30] There are several experiments that confirm this explanation. Experiments with both Er^{3+} (Ref. 26) and Eu^{3+} (Ref. 27) showed that the same anomalous cubic–to–single-pair concentration dependence occurred, even when the crystals were quenched from a high enough temperature to eliminate all clusters and other centers that could provide competing equilibria for F_i'. Experiments in $SrCl_2$ showed the same anomalous behavior in the absence of other possible competing equilibria; they also showed that the anomalous behavior vanishes at very low dopant concentrations where the activi-

ty coefficients for the nonideality corrections approach unity and no corrections are needed.[29] Experiments in PbF_2 with both Er^{3+} (Ref. 38) and Eu^{3+} (Ref. 39) showed a very dramatic and anomalous increase in the cubic site concentration and a disappearance of all other sites at the superionic transition temperature. The superionic transition is where one would expect the nonideality corrections to dominate. In fact, it was argued that the nonideality corrections in the fluorites may be driving the transition. This picture is bolstered by experiments where the transition temperature was lowered by increasing rare-earth dopant concentrations. The lowered temperature was observed by site-selective spectroscopy,[38,39] Brillouin scattering, microwave conductivity,[18] and specific heat measurements.[40] All the information shows that the presence of dopants changes the free energies for forming anion defects in a way that depends on dopant concentration. This change is consistent with nonideality corrections controlling the superionic transition.

HADES calculations were also used to provide insight into the anomalous changes in ionic conductivity that were measured by Archer et al.[41] These measurements have shown an unexplained and sudden increase in conductivity at 870 K. It was speculated that the difference in the formation energies between a neutral hexamer and a hexamer that had lost a fluoride interstitial $(6|0|8|6 \rightarrow 6|0|8|5 + 0|0|0|1)$ was small enough that the hexamer dissociation would explain the rapid conductivity increase.[15]

In this paper, we study the kinetics of the site distribution in Eu^{3+}:CaF_2. The four dominant sites are labeled by A, O, R, and Q corresponding to the tetragonal single-pair site, the cubic site, and the two cluster sites, respectively. A minor single-pair site labeled P was also observed, but the charge compensation for the site has never been determined. We first create a nonequilibrium site distribution by quenching Eu^{3+}:CaF_2 from a high temperature where the clusters have dissociated and the single-pair site has an anomalously high concentration relative to the cubic site. The crystal is then annealed at a lower temperature and the absolute concentration of all sites is followed by site-selective laser spectroscopy as the crystal relaxes to the lower-temperature site distribution. The results show the single-pair and cubic sites remain in equilibrium during the entire process. The kinetics of the relaxation are controlled by the cation dopant migration as the clusters are formed. The absolute concentrations, the rate constants for the relaxation, and the time dependences of the sites as a function of dopant concentration show the R and Q sites correspond to dimer and trimer clusters, respectively, of the form $(2Eu_{Ca} \cdot 3F_i)'$ and $(3 Eu_{Ca} \cdot 4F_i)'$ where an extra F_i' gives each center a net negative charge. These observations give strong support to the HADES calculations that predict the importance of dimers and trimers for the lighter-rare-earth dopants.[13,31] They show the dominance of F_i' scavenging and confirm the stability of the $2|0|2|3$ cluster that was predicted first in simulations by Andeen et al.[10] and later by HADES calculations.[11,12] The most stable cluster though is the trimer with an extra F_i' which is suggested to correspond to a $3|0|2|4$ cluster that has not been modeled. The struc-

ture of the $3|0|2|4$ is suggested to be directly related to the cubo-octahedral cluster by association and rearrangement of two $3|0|2|4$ clusters. The measurements also show the anomalous changes in the cubic–to–single-pair ratio observed earlier. Measurements of the equilibrium constant for the single-pair association equilibrium shows the changes expected when nonideality corrections are important.

II. EXPERIMENT

The Eu^{3+}:CaF_2 crystals were obtained commercially. The dopant concentrations were determined by neutron activation analysis. The fraction of europium ions in the divalent oxidation state was determined by uv-visible spectrophotometry. To study the aggregation kinetics of the Eu^{3+} defects, the high-temperature nonequilibrium defect distribution was formed in CaF_2 crystals doped with 0.08, 0.09, and 0.19 mol% Eu^{3+} by heating the crystals to 800–1000 °C for 9 h and quickly quenching to room temperature. The reequilibration was performed between 500 and 700 °C for up to 600 h. The samples were quenched at different times throughout the annealing process and site-selective laser spectroscopy was performed at 10 K to monitor the changes in defect site distribution. Heat treatment of the samples was accomplished by loosely wrapping the crystals in a cage of platinum wire, sealing them in an evacuated quartz tube, and heating them in a box furnace for an appropriate period of time. Small amounts of PbF_2 placed in platinum crucibles were also sealed in the evacuated tubes to act as an oxygen scavenger during heating. The samples were quenched by plunging the tubes directly from the furnace into warm water. The absence of oxygen contamination was verified by the absence of lines associated with oxygen compensation in the laser excitation spectra of the samples.

Aggregation kinetics were monitored for the three concentration samples at 562 °C. Kinetics were monitored in the CaF_2:(0.09 mol% Eu^{3+}) sample at 562, 605, and 641 °C so activation energies could be determined from the temperature dependences of the rate constants for aggregation.

A detailed description of the site-selective laser excitation technique has been presented previously.[42] A pulsed nitrogen pumped dye laser is collimated and directed through a beamsplitter to reach a sample mounted on a copper holder held at 10 K by a closed-cycle cryogenic refrigerator. The laser intensity is measured before and after the sample so that the sample absorbance can be calculated. The sample fluorescence is collected at 90° to the exciting beam. Excitation spectra of the Eu^{3+} $^7F_0 \rightarrow {}^5D_1$ transition were obtained by monitoring the fluorescence of the $^5D_0 \rightarrow {}^7F_1$ transitions. The area of single excitation peaks was measured to obtain the relative site concentrations. The peak areas were converted to Eu^{3+} site concentrations for a given defect site by fitting the data for all concentrations, annealing times, and annealing temperatures to equations of the form

$$\alpha_A I_A(t) + \alpha_O I_O(t) + \alpha_P I_P(t) + \alpha_R I_R(t) + \alpha_Q I_Q(t) = C_T$$

where the subscripts refer to the different defect sites, the α_N and $I_N(t)$ are the regression coefficients and time-dependent peak areas, respectively, for site N, and C_T is the total concentration of trivalent europium in the crystal. The details of this procedure as well as checks for its accuracy have been previously published.[27]

III. RESULTS AND DISCUSSION

Figure 2(b) shows the $^5D_1$ excitation spectrum of the 0.19 mol % Eu^{3+}: CaF_2 crystal before it had been heated and quenched. The transitions have been labeled by A, O, P, Q, and R corresponding to the five different sites previously identified. Figure 2(a) shows the same spectrum after the heating and quenching procedure. There is a dramatic change in the site distribution. Figure 3 shows the results of annealing the crystal at 562 °C for the times indicated on the figure. These spectra together with others for the different annealing temperatures and dopant concentrations were all used in the regression analysis to determine the absolute concentrations of the major sites during the annealing. The P site concentration was always small and did not change enough to permit determination of its absolute concentration. It did not appear to play an important role in determining the site distribution.

The time dependences of the absolute site concentrations are shown in Figs. 4–6 for the three different crystal concentrations. Several striking features are evident in these data. The O site concentration decreases very slowly over the time period of the experiment but the A site decreases very rapidly. The final steady state values are consistent with the anomalous increase in the equilibrium tetragonal-to-cubic site ratios observed by previous workers in experiments where crystals were quenched from increasing annealing temperatures.

The A site decrease is accompanied by a similar increase in the R site concentration. The R site later goes down in concentration as the Q site begins to grow in at
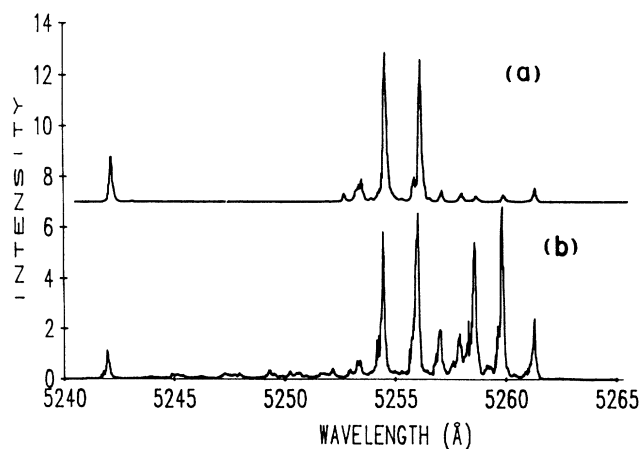
longer times. The Q site dominates at long annealing times. This behavior could not be seen in earlier equilibrium annealing studies where a low and relatively constant R site concentration was observed as a function of the annealing temperature. The qualitative features of the kinetics as well as the relationships of the absolute concentrations and the magnitudes of the rate constants must all be fit by a kinetic model for all the concentrations and temperatures used in the experiments.

FIG. 3. Excitation spectra for different annealing times (in hours) of a 0.19 mol % Eu^{3+}:CaF_2 sample at 562 °C.

FIG. 2. Laser excitation spectra of CaF_2:(0.1 mol % Eu^{3+}) (a) treated at 1250 °C and cooled quickly and (b) annealed at 600 °C for ten days. The spectra were taken by monitoring fluorescence at 590 nm with a wide spectral bandpass.
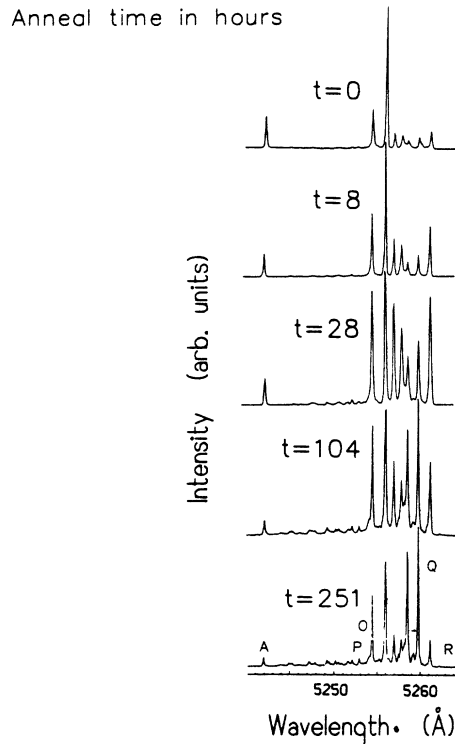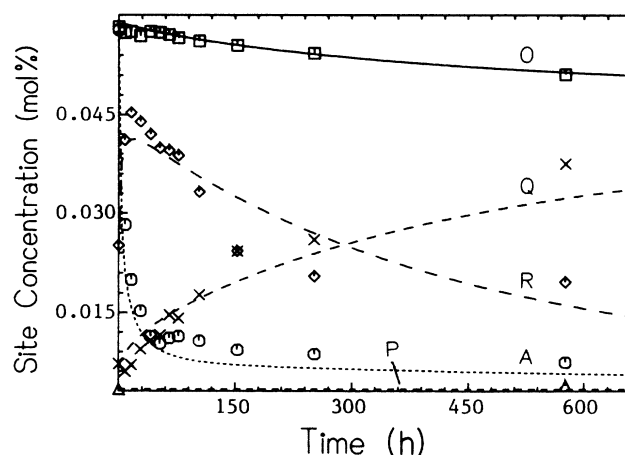

FIG. 4. Time dependence of the absolute site concentrations in a 0.19 mol % Eu^{3+}:CaF_2 crystal at 562 °C. The lines show the simulations for the concentration dependence where the R site is a 2|0|2|3 dimer and the Q site is a 3|0|2|4 trimer.
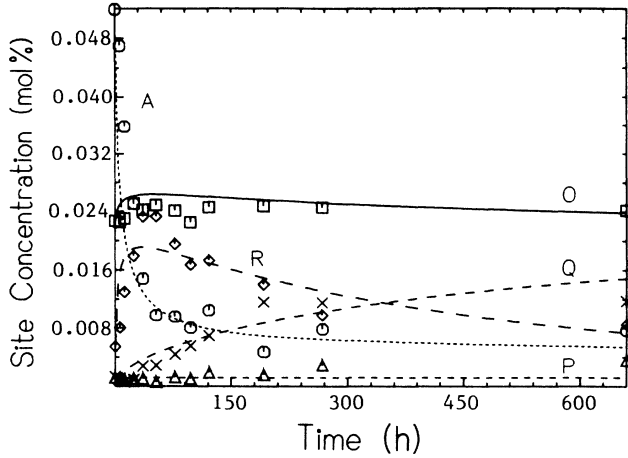
FIG. 5. Time dependence of the absolute site concentrations in a 0.09 mol % Eu^{3+}:CaF_2 crystal at 562 °C. The lines show the simulations for the concentration dependence where the R site is a 2|0|2|3 dimer and the Q site is a 3|0|2|4 trimer.

Kinetic simulations were performed to match the experimental data. A large number of different models and mechanisms were tried where the R and Q centers were assigned between one and six Eu^{3+} ions and between one and eight F_i^- ions. Only the model shown below provided reasonable fits to the data for all concentrations and temperatures:
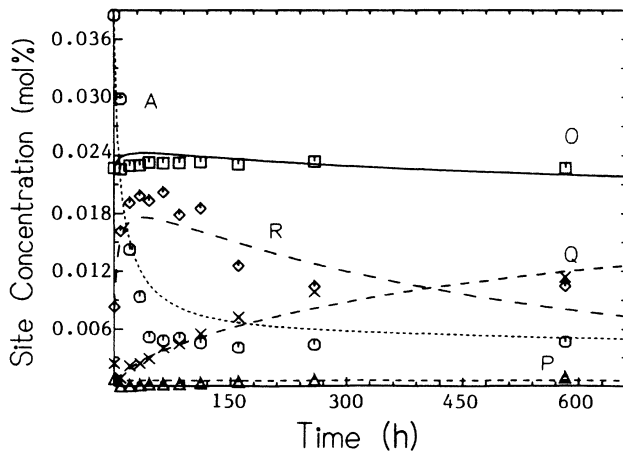
$$O + F_i \underset{k_{-1}}{\overset{k_1}{\rightleftarrows}} A \ , \tag{1}$$

$$A + A + F_i \underset{k_{-2}}{\overset{k_2}{\rightleftarrows}} R \ , \tag{2}$$

$$R + A \underset{k_{-3}}{\overset{k_3}{\rightleftarrows}} Q \tag{3}$$

FIG. 6. Time dependence of the absolute site concentrations in a 0.08 mol % Eu^{3+}:CaF_2 crystal at 562 °C. The lines show the simulations for the concentration dependence where the R site is a 2|0|2|3 dimer and the Q site is a 3|0|2|4 trimer.

where charge neutrality has been used to fix $[F_i'] = [O] - [R] - [Q]$. The fits to the data are shown as the lines in Figs. 4–6. Table I summarizes the values used in the fitting. The agreement between the kinetic models and experimental data is quite good and confirms the model. The A site decreases rapidly while the R site increases rapidly since the single-pair centers cluster to form dimers. The cubic site concentration does not decrease at the same time because the dimers require an extra F_i' that is extracted from the single pairs to form cubic sites. The Q site increases over a longer time period because it requires formation of the R site. The Q site increase is therefore correlated with the R site decrease at longer annealing times.

There are several relevant comments about the model. The second step probably corresponds to a slow step where two A centers interact followed by a rapid step where the F_i' equilibrates with the dimer. A key point of the model is k_1 and k_{-1} are very fast compared with the other rate constants so the F_i' are in equilibrium with all centers. The ratio of rate constants is defined by

$$K = k_1 / k_{-1} = [A] / [O][F_i'] \ . \tag{4}$$

Rapid equilibration involving F_i migration and slow rates involving cation migration are consistent with previous work in this system. In fact, previous work suggests that cation migration should be so slow that it would not be observable in these experiments,[43] a result that is inconsistent with the changes in the cluster site concentrations observed in this work. The differences in the two experiments may reflect whether the cation diffusion occurs over macroscopic distances required for diffusion measurements or over distance scales on the order of the separation between centers involved in this work.

Since the cubic site (O) concentration decreases slowly while the single-pair site (A) decreases rapidly, it is reasonable to expect the F_i' concentration must also be decreasing to maintain the equilibrium between A and O as defined in Eq. (4). The model accounts for the rapid F_i' decrease with the incorporation of F_i' scavenging by the R and Q sites. Both must be scavenging in order to maintain the low F_i' concentrations over the entire annealing

TABLE I. (a) Fitting parameters for concentration dependence at 562 °C and (b) fitting parameters for temperature dependence of 0.09 mol % crystal.

(a)	
$K = k_1/k_{-1}$ (0.08 mol % crystal)	200 mol %$^{-1}$
(0.09 mol % crystal)	160 mol %$^{-1}$
(0.19 mol % crystal)	50 mol %$^{-1}$
k_2	120 h^{-1} mol %
k_{-2}	0.001 h^{-1}
k_3	22 h^{-1} mol %$^{-1}$
k_{-3}	8.0×10^{-5} h^{-1}

(b)		
Activation energy	R site	0.49 ±0.08 eV
	Q site	1.5 ±0.4 eV

time. Otherwise, the O site concentration would decrease. The Q site does not grow until substantial amounts of the R cluster have formed. If both R and Q were dimers (or other clusters with the same number of Eu^{3+} ions) differing only in the F_i' ions, the high F_i' mobility would cause interconversion. Finally, the optimum fit for all dopant concentrations requires the R and Q sites to be dimers and trimers, respectively.

Table I shows that different values are required for the equilibrium constant to fit the data for each concentration crystal. If the equilibrium values for the A and O site concentrations were described by a mass-action relationship, the values should not change. The differences are attributed to the nonideality corrections that have been observed in previous work. The corrections account for the anomalous increase in the cubic-to-tetragonal single-pair ratio as the dopant concentration increased, even when the crystals had been quenched from high temperatures to eliminate competing equilibria from clusters. The sizes of the nonideality corrections required to describe the data are consistent with previous work.[27-29]

There are systematic deviations in the shape of the R site kinetics primarily because the R site concentration decays more rapidly than the model predicts. Attempts to match the shape of the curve more closely lead to larger departures for other sites. The deviations may be experimental error but are more likely inadequacies in the model. The kinetic model assumed that each step in the mechanism could be described by mass-action relationships, which is inconsistent with the fact that nonideality corrections are known to be important. On the other hand, there is no appropriate way to correctly include the activity effects in the kinetics. We must assume that the activity effects do not change appreciably during the experiment. This assumption may be questionable in the region where the large charged clusters are forming.

Experiments were also performed with the 0.09 mol % Eu^{3+}:CaF_2 crystal for different temperatures over the

FIG. 8. Time dependence of the absolute site concentrations in a 0.09 mol % Eu^{3+}:CaF_2 crystal at 605 °C. The lines show the simulations for the temperature dependence where the R site is a 2|0|2|3 dimer and the Q site is a 3|0|2|4 trimer.

range from 562–641 °C in order to determine the activation energy of the defect aggregation. Figures 7–9 show the kinetic data for all the sites along with the fitted curves using the same model described earlier. Table I summarizes the activation energies that were determined from the fitting procedure. Although there are no theoretical calculations for comparison, the values are typical of activation energies measured in the fluorites.

There have been a number of speculations that F_i' scavenging occurs by formation of a $[M_{Ca} \cdot 2F_i]'$ center (where M is a rare earth) (Refs. 12, 36, and 37) and calculations that confirm the stability of such a center.[12] There is no evidence in this study that supports a single-pair scavenging center. The A site cannot be this center for several reasons. The kinetic behavior, concentration, and temperature dependence are all opposite from that required for a scavenging center. At short anneal times,
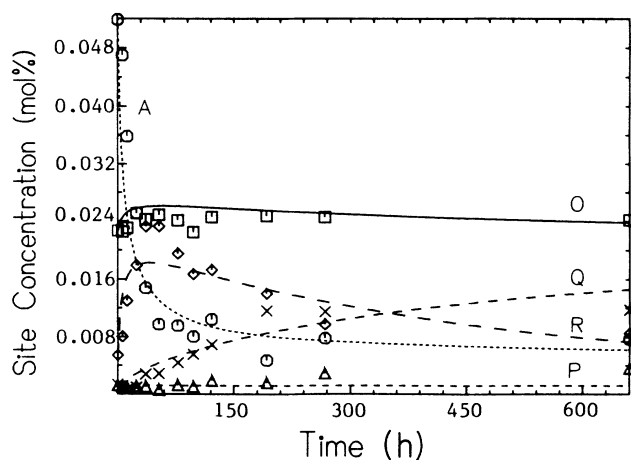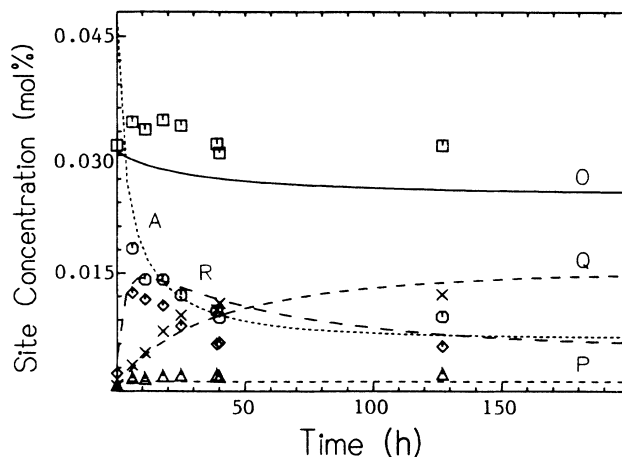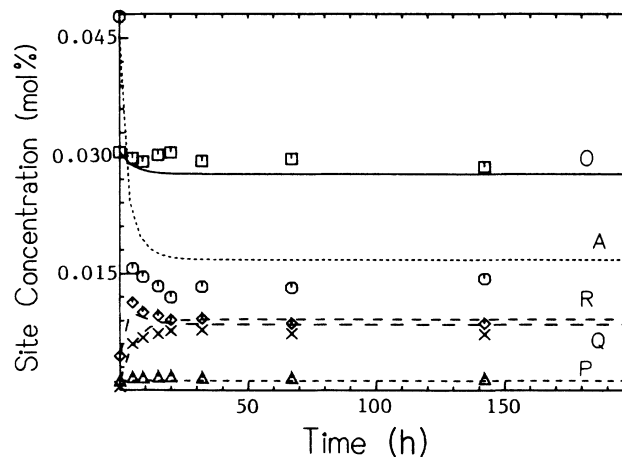

FIG. 7. Time dependence of the absolute site concentrations in a 0.09 mol % Eu^{3+}:CaF_2 crystal at 562 °C. The lines show the simulations for the temperature dependence where the R site is a 2|0|2|3 dimer and the Q site is a 3|0|2|4 trimer.

FIG. 9. Time dependence of the absolute site concentrations in a 0.09 mol % Eu^{3+}:CaF_2 crystal at 641 °C. The lines show the simulations for the temperature dependence where the R site is a 2|0|2|3 dimer and the Q site is a 3|0|2|4 trimer.

the A site has twice the concentration of the O site and, hence, would require substantial F$'_i$ scavenging from anion lattice sites. In addition, the L-shaped geometry of the center calculated by Catlow and co-workers[11] to be most stable or the trigonal symmetry proposed by Welsh[36] are inconsistent with the tetragonal symmetry of the A site. Similarly, there is no indication that the P site corresponds to this center since its time dependence does not reflect the required changes in the F$'_i$ concentration.

The $2|0|2|3_1$ dimer cluster shown in Fig. 1 for the R site was proposed by Andeen et al. on the basis of simulations.[10] The trimer structure proposed for the Q site in Fig. 1 is derived from the $2|0|2|3_1$ cluster. The $2|0|2|3_1$ cluster has two compensating F$'_i$ ions in the Eu^{3+} plane. These ions displace the two lattice F$^-$ ions located between the Eu^{3+} ions into interstitial positions above and below the Eu^{3+} ions. In the figure, an additional F$'_i$ is scavenged and fits into the second interstitial position above the Eu^{3+} ions. The final $2|0|2|3_1$ structure therefore has an asymmetry between the two F$'_i$ above the Eu^{3+} and the one below it. The proposed $3|0|2|4$ trimer in Fig. 1 has a symmetrical structure for the two F$'_i$ both above and below the Eu^{3+} ions. It is formed by adding a tetragonal single-pair center to the bottom layer of the dimer so the three Eu^{3+} ions lie in a (111) plane and the F$'_i$ fills the second interstitial position in the bottom layer. This structure is then consistent with the $6|0|8|6$ cubo-octahedral cluster which can be formed by the reaction

$$2(3|0|2|4) \rightleftharpoons 6|0|8|6 + 2(0|0|0|1) \ .$$

The structure of the $6|0|8|6_1$ cluster can be formed by the superposition of two $3|0|2|4$ clusters followed by the relaxation of four remaining lattice F$^-$ ions into interstitial positions and the expulsion of two F$'_i$ ions.[15] It is actually not clear that the two F$'_i$ ions are expelled because the earlier site-selective spectroscopy in the heavier-rare-earth dopants showed that scavenging must persist, even at high concentrations. In fact, it must occur with increasing efficiency at the higher concentrations in order to describe the continuing decrease in the single-pair site concentrations at higher concentrations.[26] The presence of extra F$'_i$ would explain several other observations. The proposed $6|0|8|6_1$ structure is symmetrical and unique. Extra F$'_i$ would destroy the symmetry and lead to the formation of many new centers differing in the relative placement of the extra F$'_i$. This prediction agrees with the many different sites labeled $D1$(a)–1(k) or $D2$(a)–2(d) seen in previous work by site-selective spectroscopy.[44] It also agrees with the observation that the cluster has a macroscopic dipole moment. Dielectric measurements by Andeen et al. show the R_{III} dielectric relaxation peak correlates with the $D2$(a) site and therefore with the hexamer cluster.[10] This relaxation would not have been observed if the hexamer had the symmetrical $6|0|8|6_1$ structure. This evidence strongly suggests that there are even more than the six F$'_i$ ions in the cubo-octahedral clusters than have been considered thus far. These additional F$'_i$ are probably being added to the $6|0|8|6_1$ cluster because neighboring pairs of F$'_i$ ions in the top layer of Fig. 1(e) displace F$^-$ ions from their normal positions to intersti-

tial positions in the next layer up. Lattice strains are created that could provide the driving force for the scavenging of an additional F$'_i$ ion above the top Eu^{3+} in the figure to create a $6|0|9|7$ cluster. This model invokes the same F$^-$ displacements as the $2|0|2|3_1$ cluster. Displacements of all four equivalent F$^-$ in normal lattice positions on the top layer would create a $6|0|12|7$ cluster. Since the same diplacements could occur on any face of the hexamer, up to six F$'_i$ could conceivably be added to the cluster. This fully gettered $6|0|32|12$ hexamer is sketched in Fig. 10. The relative importance of hexamers with the form $6|0|(8+4n)|(6+n)$ where n is an integer from 1 to 6 will depend both on the formation energies, dopant concentrations, and dopant ionic radii.

The changes in relative importance of dimers, trimers, and hexamers in CaF$_2$ as the dopant ion is changed from lighter to heavier rare earths can be understood from the work of Andeen et al. The R_{III} relaxation peak that corresponds to the hexamers is present for Tb^{3+} and heavier rare earths. The R_{IV} relaxation that corresponds to either the dimer or trimer is present for all the rare earths
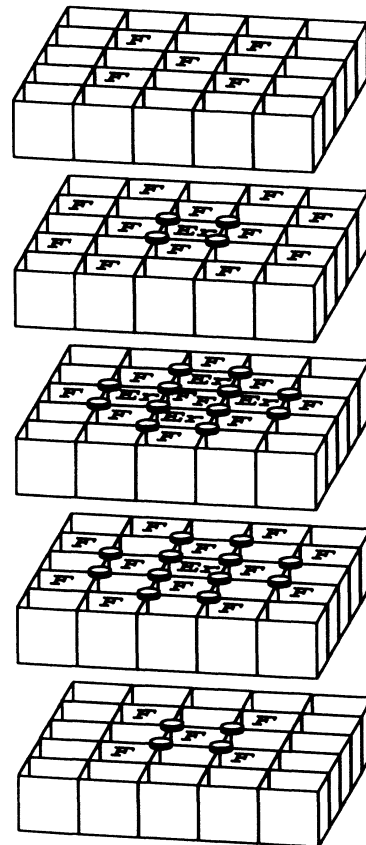

FIG. 10. Exploded three-dimensional representation of the proposed $6|0|32|12$ hexamer cluster structure that may be important for the heavier rare earths like Er^{3+}. The line intersections represent normal fluoride lattice sites while Ca^{2+} ions (not shown) occupy alternate cube center positions. The fluoride interstitial and Er^{3+} ions are shown explicitly and fluoride vacancies are indicated by disks at line intersections. There are two fluoride interstitials in the very center of the structure.

lighter than Tm^{3+}. The R_{VII} and R_{VI} relaxations occur for the intermediate rare earths including Sm^{3+}, Eu^{3+}, and Gd^{3+} with the R_{VII} being more dominant. If the R_{IV} relaxation corresponds to the dimer and the R_{VII} relaxation corresponds to the trimer, there would be a clear progression where the dimer occurs for the light rare earths, the dimer and trimer occur for intermediate rare earths, and the hexamer occurs for the heavy rare earths. This order is consistent with the HADES simulations as well. In all cases, the clusters contain extra F_i' to provide the scavenging observed in all the systems.

IV. CONCLUSIONS

This work has resulted in a more complete and detailed description of the fluorite defect chemistry than is possible with other approaches. F_i' scavenging is accomplished by forming $2|0|2|3_1$ and $3|0|2|4_1$ clusters, with no evidence of scavenging by forming $1|0|1|2$ sites. The dimers and trimers are related to the hexamers that have been proposed previously. It is pointed out that the hexamers must also be scavenging F_i' ions and are probably forming clusters of the form $6|0|(8+n)|(6+n)$ or $6|0|(8+4n)|(6+n)$. The large number of possibilities agrees with laser measurements that there are many different sites associated with the large clusters.

The site-selective kinetic measurements are a particularly powerful way to test the predictions of the HADES modeling of clusters in fluorite structure materials. The previous work that uses EXAFS to determine the nature of defect clustering is not sensitive to small differences in the makeup of clusters and is not able to distinguish between the different clusters that have been shown to be present. Only an ensemble average of the electron scattering from all sites is observed in EXAFS. This work has provided the first detailed insights into the nature of clustering in the fluorites. It provides striking confirmation to the prediction that dimers and trimers dominate for light-rare-earth dopants and that F_i' scavenging by clusters is favorable. Calculations must still be performed on the proposed $3|0|2|4_1$ trimer and its relationship to the other centers must be established. It is also necessary to extend the calculational methods to the case where strain interactions can be correctly modeled, both to understand their role in superionic conductivity and their influence on determining the site distributions. At that point, it may be possible to extend the theoretical capabilities past calculations of stability to the point where predictions can be made for how the distributions change under different conditions of crystal doping and annealing. For example, calculations predict that many centers would be stable in $Eu^{3+}:CaF_2$ but only four dominate because the relative free energies, center concentrations, and temperature conditions determine the actual defect distribution. The information reported in this work would serve as an excellent test for the development of theoretical models that could predict the defect distributions.

These results are also relevant to the mechanism for the rapid increase in ionic conductivity found by Archer et al.[41] The suggestion that the increase was caused by dissociation of a neutral hexamer was based on calculations that did not consider the possibility of a charged cluster. A cluster with extra F_i' ions could perhaps readily lose the F_i' and account for the rapid conductivity increase.

*Present address: Aluminum Company of America, Alcoa Center, PA 15069.

†Author to whom correspondence should be sent.

[1]C. R. A. Catlow, M. J. Norgett, and T. A. Ross, J. Phys. C **10**, 1627 (1977).

[2]A. N. Cormack, in *Defects in Solids*, Vol. 147 of *NATO Advanced Study Institute, Series B: Physics*, edited by A. V. Chadwick and M. Terenzi (Plenum, New York, 1986), p. 51.

[3]J. H. Harding, in *Defects in Solids* Vol. 147 of *NATO Advanced Study Institute, Series B: Physics*, edited by A. V. Chadwick and M. Terenzi (Plenum, New York, 1986), p. 303.

[4]A. B. Lidiard, in *Crystals with the Fluorite Structure*, edited by W. Hayes (Clarendon, Oxford, 1974).

[5]A. V. Chadwick, in *Defects in Solids*, Vol. 147 of *NATO Advanced Study Institute, Series B: Physics*, edited by A. V. Chadwick and M. Terenzi (Plenum, New York, 1986), p. 37.

[6]C. R. A. Catlow, J. Phys. C **6**, L64 (1973).

[7]C. R. A. Catlow, J. Phys. C **9**, 1845 (1976).

[8]C. R. A. Catlow, J. Phys. C **9**, 1859 (1976).

[9]C. R. A. Catlow, M. J. Norgett, and T. A. Ross, J. Phys. C **10**, 1627 (1977).

[10]C. G. Andeen, J. J. Fontanella, M. C. Wintersgill, P. J. Welcher, R. J. Kimble, and G. E. Matthews, J. Phys. C **14**, 3557 (1981).

[11]J. Corish, C. R. A. Catlow, P. W. M. Jacobs, and S. H. Ong, Phys. Rev. B **25**, 6425 (1982).

[12]C. R. A. Catlow, A. V. Chadwick, and J. Corish, J. Solid State Chem. **48**, 65 (1983).

[13]P. J. Bendall, C. R. A. Catlow, J. Corish, and P. W. M. Jacobs, J. Solid State Chem. **51**, 159 (1984).

[14]P. J. Bendall, C. R. A. Catlow, and B. E. F. Fender, J. Phys. C **17**, 797 (1984).

[15]C. R. A. Catlow, A. V. Chadwick, J. Corish, L. M. Moroney, and A. N. O'Reilly, Phys. Rev. B **39**, 1897 (1989).

[16]S. F. Matar, J. M. Reau, P. Hagenmuller, and C. R. A. Catlow, J. Solid State Chem. **52**, 114 (1984).

[17]C. R. A. Catlow, R. T. Harley, and W. Hayes, J. Phys. C **10**, L559 (1977).

[18]C. R. A. Catlow, J. D. Comins, F. A. Germano, R. T. Harley, W. Hayes, and I. B. Owen, J. Phys. C **14**, 329 (1981).

[19]C. W. Rector, B. C. Pandey, and H. W. Moos, J. Chem. Phys. **45**, 171 (1966).

[20]R. W. Ure, J. Chem. Phys. **26**, 1363 (1957).

[21]A. D. Franklin and S. Marzullo, Proc. Brit. Ceram. Soc. **19**, 135 (1971).

[22]G. K. Miner, T. P. Graham, and G. T. Johnston, J. Chem. Phys. **57**, 1263 (1972).

[23]J. M. O'Hare, T. P. Graham, and G. T. Johnston, J. Chem. Phys. **61**, 1602 (1974).

[24]A. D. Franklin, J. Chem. Phys. **64**, 1509 (1976).

[25]P. P. Yaney, D. M. Schaeffer, and J. L. Wolf, Phys. Rev. B **11**, 2460 (1975).

[26]D. R. Tallant, D. S. Moore, and J. C. Wright, J. Chem. Phys. **67**, 2897 (1977).

[27]R. J. Hamers, J. R. Wietfeldt, and J. C. Wright, J. Chem. Phys. **77**, 683 (1982).

[28]D. S. Moore and J. C. Wright, J. Chem. Phys. **74**, 1626 (1981).

[29]J. R. Wietfeldt and J. C. Wright, J. Chem. Phys. **86**, 400 (1987).

[30]J. C. Wright, Cryst. Lattice Defects Amorph. Mater. **12**, 505 (1985).

[31]C. R. A. Catlow, A. V. Chadwick, G. N. Greaves, and L. M. Moroney, Nature (London) **312**, 601 (1984).

[32]D. S. Moore and J. C. Wright, Chem. Phys. Lett. **66**, 173 (1979).

[33]W. Gettman and O. Greis, J. Solid State Chem. **26**, 255 (1978).

[34]D. J. M. Bevan and O. Greis, Rev. Chim. Miner. **15**, 346 (1978).

[35]O. Greis, Rev. Chim. Miner. **15**, 481 (1978).

[36]H. K. Welsh, J. Phys. C **18**, 5637 (1985).

[37]J. H. Crawford and G. E. Matthews, Semicond. Insul. **2**, 213 (1977).

[38]S. I. Mho and J. C. Wright, J. Chem. Phys. **79**, 3962 (1983).

[39]F. J. Weesner, J. C. Wright, and J. J. Fontanella, Phys. Rev. B **33**, 1372 (1986).

[40]H. W. den Hartog and J. van der Veen, Phys. Rev. B **37**, 1807 (1988).

[41]J. A. Archer, A. V. Chadwick, I. R. Jack, and B. Zegiri, Solid State Ionics **9&10**, 505 (1983).

[42]M. P. Miller, D. R. Tallant, F. J. Gustafson, and J. C. Wright, Anal. Chem. **49**, 1474 (1977).

[43]M. Baker and A. Taylor, J. Phys. Chem. Solids **30**, 1003 (1969).

[44]D. R. Tallant and J. C. Wright, J. Chem. Phys. **63**, 2074 (1975).